Molecular Spin-Flip Loss and a Dual Quadrupole Trap

David Reens,* Hao Wu,* Tim Langen,† and Jun Ye
JILA, National Institute of Standards and Technology and the University of Colorado and Department of Physics, University of Colorado, Boulder, Colorado 80309-0440, USA
(Dated: August 13, 2017)

Doubly dipolar molecules exhibit complex internal spin-dynamics when electric and magnetic fields are both applied. Near magnetic trap minima, these spin-dynamics lead to enhancements in Majorana spin-flip transitions by many orders of magnitude relative to atoms, and are thus an important obstacle for progress in molecule trapping and cooling. The effect is strongest for Hund's case (a) states and is significant for Hund's case (b) as well. We study these internal spin-dynamics with OH molecules and devise a trap geometry where spin-flip loss can be tuned from over 200 s^{-1} to below our 2 s^{-1} vacuum limited loss rate with only a simple external bias coil and with no sacrifice of trap strength.

The ultracold regime extends toward molecules on many fronts [1]. KRb molecules have reached lattice quantum degeneracy [2] and other bialkalis continue to progress [3–6]. Creative and carefully engineered laser cooling strategies are tackling certain nearly vibrationally diagonal molecules [7–13]. A diverse array of alternative strategies have succeeded to greater or lesser extents on other molecules [14–20]. All of these molecules will require secondary strategies like evaporation or sympathetic cooling to make further gains in phase space density [21–23]. They also may face a familiar challenge: spin flip loss near the zero of a magnetic trap, but dramatically enhanced for many doubly dipolar molecules due to their internal spin dynamics in mixed electric and magnetic fields.

The knowledge of spin flips or Majorana hops as an eventual trap lifetime limit predates the very first magnetic trapping of neutrals [24]. Spin flips were directly observed near 50 μK and overcome with a time-orbiting potential trap [25] and a plugged dipole trap [26], famously enabling the first production of Bose-Einstein condensates. Motivated by the interest in dipolar molecules in mixed fields for quantum chemistry, precision measurement and many-body physics, we previously investigated loss of magnetically trapped hydroxyl radicals (OH) with applied electric field [27]. This trap loss occurred for substates of OH's $X^2\Pi_{J=3/2}$ ground state manifold other than the most well trapped one (positive parity and full spin polarization, $|f, m_J = 3/2\rangle$, blue in Fig. 1). Due to the closely spaced parity doublet, a general feature of Hund's case (a), these states intersect opposite parity states at non-zero B-fields, where E-field can open avoided crossings and cause trap loss. We now identify internal spin-dynamics leading to trap loss near $B = 0$ even for the most well trapped state and even at 50 mK.

These internal spin-dynamics are subtle, having eluded three previous investigations of note: In [28] the analogues of atomic spin-flip loss for molecules in mixed fields were modeled, and a magnetic quadrupole trap for OH molecules with superposed E-field was specifically addressed. It was concluded that no significant loss enhancement due to electric field would be evident. This is true only for the approximate $^2\Pi_{1/2}$ Hamiltonian used in that study. In [29] E-fields were applied in our magnetic quadrupole trap to study E-field induced collisions. Although an initial approximation was made of the spin-dynamical effect, subsequent investigations have revealed it to be a threefold underestimate, enough to render de-

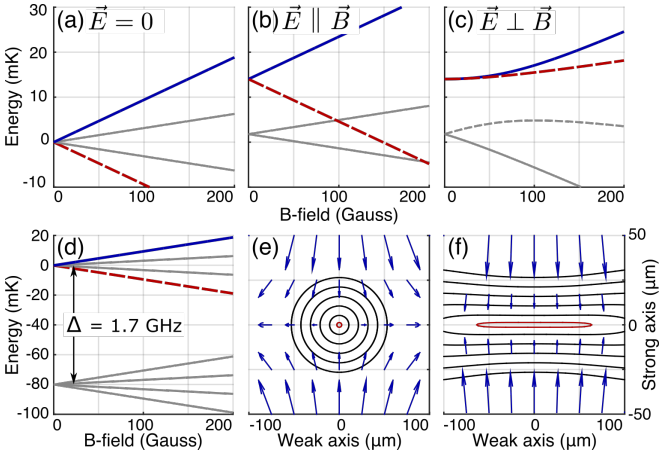

FIG. 1. A uniform E-field, added to magnetically trapped molecules for dipolar studies or other purposes, can lead to spin-flip losses. Four Zeeman split lines in OH's $X^2\Pi_{3/2}$ manifold are shown (a-c), with the trapped $|f, 3/2\rangle$ state in blue and its spin-flip partner $|f, -3/2\rangle$ in dashed red. These states are shown with no E-field (a), with $E = 150$ V/cm and $E \parallel B$ (b), and with $\vec{E} \perp \vec{B}$ (c). Note the vastly reduced red-blue splitting in the latter case. The gray close dashes (c) denote the $|f, 1/2\rangle$ state, which is briefly discussed in the main text. The opposite parity ($|e\rangle$) manifold is split by Δ (d). Energy splitting contours are shown every 40 MHz near the zero of a 2 T/cm magnetic quadrupole trap for OH molecules [27] without E-field (e), and with uniform $E = 150$ V/cm along the strong axis of the quadrupole (f). The vectors are $\mu_{\text{eff}}\vec{B} \pm d_{\text{eff}}\vec{E}$, where the sign is positive above the horizontal centerline and negative below, which represents the proper quantization axis for magnetically trapped molecules. Note the drastic widening of the lowest contour (red), the culprit for molecular spin-flip loss enhancement.

convolution of any remaining collisional effect difficult. Finally, in [30] it was correctly noted that Hund's case (a) molecules maintain a quantization axis in mixed fields. The states of the molecule were shown to align with one of the two quantization axes given by the vectors $\mu_{\text{eff}}\vec{B} \pm d_{\text{eff}}\vec{E}$, μ_{eff} and d_{eff} the effective dipole moments of the molecule in uncombined fields. It was asserted that this would maintain quantization near the zero of a quadrupole trap and avoid spin-flip loss, but as we now describe the loss is actually enhanced.

We begin with an intuitive explanation of the loss enhancement based on molecular orientation. Consider a magnetic quadrupole trap, where a weak-field seeking molecule remains trapped insofar as it adiabatically follows the field direction. When molecules pass near the trap center, they experience a rotating field direction, causing spin-flips. When electric field is added, it dominates in the trap center where the magnetic field is weakest. As correctly noted in [30], this causes a quantization axis to be maintained, either of $\mu_{\text{eff}}\vec{B} \pm d_{\text{eff}}\vec{E}$. Now suppose a molecule initially follows the sum quantization axis and is in a region where E and B are nearly parallel before passing by the trap center. After passing the trap center, B rotates nearly 180°, so that E and B are nearly anti-parallel. Now the length of the sum quantization axis, which is proportional to the field induced energy shift of the molecule, actually decreases with increasing $|B|$. Further away from the trap center the molecule is then magnetically strong field seeking and is lost. To be more general, we define the relative orientation of the fields as the sign of $\phi = \vec{E} \cdot \vec{B}$. When ϕ is negative, the trapped state must have the vector difference quantization axis, and vice versa, so that an increase in magnitude of the magnetic field increases internal energy. Whenever ϕ changes sign, i.e. where $\phi = 0$ and $\vec{E} \perp \vec{B}$, there will be a chance of spin-flip associated with the molecule's propensity to maintain its quantization axis rather than remain on the highest energy doubly weak field seeking branch. Since ϕ is a continuous scalar defined in 3D, $\phi = 0$ is one of it's contour levels and thus always corresponds to a 2D surface; in the case of a magnetic quadrupole with homogeneous E it is a plane.

This intuition is in agreement with a more rigorous analysis of the energy splittings between the trapped state and its spin-flip partner. By exactly diagonalizing the approximate eight state ground molecular Hamiltonian for OH, subtracting the relevant state energies and Taylor expanding, we find:

$$H(B_\perp, B_{||}, E) = (\mu_{\text{eff}} B_\perp)^3 \Lambda^2 / (d_{\text{eff}} E)^4 + \mu_{\text{eff}} B_{||} \quad (1)$$

Here the magnetic field is considered in parallel and perpendicular components relative to the electric field, and Λ is the lambda doubling. The relevant splitting between spin flip partner states reaches a deep minimum whenever $B_{||}$ goes to zero and $\vec{E} \perp \vec{B}$, where the remaining Zeeman splitting is reduced from linear to cubic in magnetic field (Fig. 1a-c). This reduction in the Zeeman splitting from linear to cubic is in fact a well known phenomenon in the precision measurement community, and experimentalists have exploited it for the suppression of unwanted influence from magnetic fields in measurements of the electron electric dipole moment. However, in the case of applying mixed fields during trapping, this suppression is not beneficial but rather detrimental, because the reduced splitting greatly expands the region in which spin-flips can occur (Fig. 1e-f). The extent of the loss enhancement is best addressed as discussed below, but a reasonable scaling law can be formed by comparing the surface area of energy contours such as those shown in red in Fig. 1e-f. For κ the energy scale of hops without any application of field, electric field enhances the loss rate by $\eta = (d_{\text{eff}} E / \sqrt{\kappa \Delta})^{8/3}$.

We can better quantify the extent of the expansion by considering molecular trajectories in light of the Landau Zener formula:

$$P_/texthop = \exp -\Delta^2 / \hbar \dot{H} \quad (2)$$

Which relates the probability of diabatically hopping between two states $P_/texthop$ to the energetic coupling between the states Δ and the rate of approach of the energy levels $\dot{H}$. Any molecules whose trajectory passes through the $\vec{E} \perp \vec{B}$surface experience a minimum energy splitting Δ at the point of intersection with the plane. The rate of approach of the levels $\dot{H}$ near this intersection is given simply by the projection of the molecule velocity on the normal to the plane, which dominates over the parallel contribution except for molecules moving almost entirely in that direction, an unlikely situation. Moreover, although the Landau-Zener formula assumes infinitely linear energy level approach before and after a crossing, the very small cubically suppressed energy gap at the crossing is dominated by the average energy of a trapped molecule, so that to a good approximation its velocity hardly changes in the regime where the energy splitting is small. With these simplifying observations, it becomes possible to approximate the hopping probability for a molecule knowing only its crossing point and orthogonal velocity. By assuming a thermal distribution, the Landau Zener probability can be numerically integrated over the instantaneous spatial distribution in the plane and the Maxwellian velocity distribution orthogonal to the plane to obtain a spin-flip loss flux out of the trap. We perform such integrations for OH in our previous 2 T/cm magnetic quadrupole [31] under various electric fields of interest (Tab. I). The results lead to important modifications of our interpretation of previous work, which we discuss further in the supplementary materials.

Generalizing beyond OH, Hund's case (a) states exhibit reduced Zeeman splittings near $B = 0$ when $\vec{E} \perp \vec{B}$ that are not always cubic as for OH but satisfy $H_{\vec{E} \perp \vec{B}}(B) \propto (\mu_{\text{eff}} B)^{2 m_J}$. Only states with $m_J = 1/2$ retain a linear Zeeman splitting, but they are either not

TABLE I. Enhancements (η) and loss rates (Γ) for OH with typical applied fields. Zero field values are equivalent to atomic spin-flip loss. E-field is required during evaporation and spectroscopy to open avoided crossings for $|e\rangle$ parity states [22, 27], or applied for polarization of the molecules to study collisions [29]. Background loss is 2 s^{-1}, experiment length 100 ms.

E (V/cm)	55 mK		5 mK		Purpose
	η	$\Gamma\,(s^{-1})$	η	$\Gamma\,(s^{-1})$	
0	1	0.02	1	1.3	Zero Field
300	5	0.1	9	11	Evaporation
550	17	0.3	40	50	Spectroscopy
3000	1000	19	1600	2000	Polarizing

well trapped if $J=1/2$ also, or they are initially linear until avoided crossings with other states (c.f. Fig. 1c). This bears out in all test Hamiltonians we have diagonalized, and can be understood intuitively as follows: the Zeeman effect is a perturbation on a Hamiltonian whose quantization axis, which defines the $|m_J\rangle$ quantum number, has already been set by the Stark effect. Normally the Zeeman effect would linearly split states according to $|m_J\rangle$, but from its perspective the states are superpositions $|m_J\rangle \pm |-m_J\rangle$ and do not split at all to first order. Only via perturbations of the eigenbasis itself does a Zeeman splitting emerge.

Beyond Hund's case (a), any state exhibiting competition between E-fields and B-fields for alignment of the molecule will be susceptible. One way to avoid competition is for the fields to couple to unrelated parts of the Hamiltonian, which happens to a limited extent for Hund's case (b) states without electron orbital angular momentum (Σ states, $\Lambda=0$) [30]. In these states, which include most laser-cooled and bialkali molecules thus far, the E-fields and B-fields couple to rotation and spin respectively, which are only related by the spin-rotation coupling constant γ. Unfortunately γ is usually in the tens of MHz, enough that molecular spin-flip loss remains quite significant. The inclusion of hyperfine requires a careful case-by-case investigation. For OH, it would initially seem to add an extra splitting that could protect from spin-flips, but in fact the lossy plane is only shifted slightly away from $\vec{E}\perp\vec{B}$but retains the same area. For YO [32], certain hyperfine states avoid spin-flip loss entirely. These states are characterized by significant electron-spin-to-nuclear-spin dipolar coupling, which results in a protective gap regardless of field orientation. Although our focus has been spin-flips in magnetic traps, spin-flips in electric traps are also possible, (cite meijer).

We can generalize to arbitrary geometries and consider methods to suppress the loss using a simple strategy: avoid $\mu_{\rm eff}B < d_{\rm eff}E$ where $\vec{E}\perp\vec{B}$. One way to achieve this is to trap with E-field and superpose B-field. The lambda doublet prevents flips in this configuration, but it correspondingly rounds the trap minimum, weakening

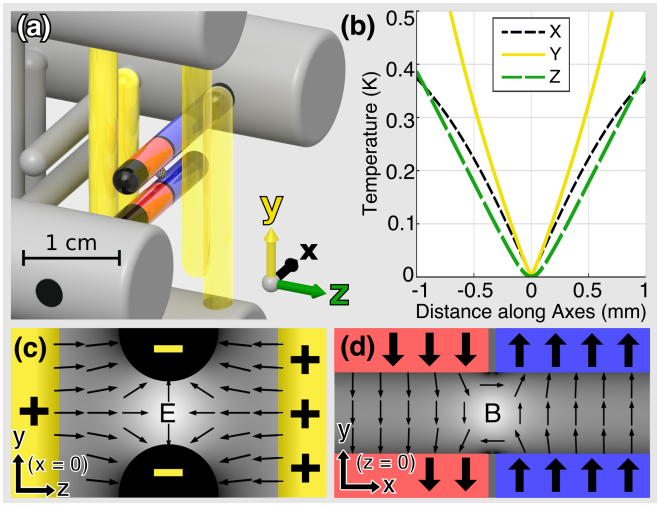

FIG. 2. The last six pins of our Stark decelerator [31] form the trap (a), which is 0.45 K deep with trap frequency $\nu\approx 4$ kHz (b). Along y the trap is bounded by the 2 mm pin spacing. The yellow pins are positively charged and the central pin pair negatively, which forms a 2D electric quadrupole trap with zero along the x-axis. This is shown for the $x=0$ plane (c), with yellow pins artificially projected for clarity since they don't actually intersect the plane. The central pins are magnetized, with two domains each. Blue indicates magnetization along $+\hat{y}$, red along $-\hat{y}$. These domains produce a magnetic quadrupole trap with zero along the z-axis, shown in the $z=0$ plane (d).

confinement. Another option is to trap with both fields and keep zeros precisely overlapped. This was realized for OH with a superposed magnetic quadrupole and electric hexapole [33]. Such a scheme prevents loss enhancement, but does not remove it entirely. Another possibility is to use one field only, but any experiment which aims to make use of the doubly dipolar nature of molecules cannot accept this compromise.

We opt for a new geometry: a pair of 2D quadrupole traps, one magnetic and the other electric, with orthogonal centerlines (Fig. 2). We achieve these fields in a geometry that matches our Stark decelerator [16]. This approach is similar to the Ioffe-Pritchard strategy [34], where a 2D magnetic quadrupole is combined with an axial magnetic dipole trap. While this successfully prevents spin-flip loss, axial and radial trapping interfere, resulting in significantly lower trap depths than for a 3D quadrupole. We thwart this interference by using electric field for the third direction. Our geometry has $\vec{E}\perp\vec{B}$ in the two planes $x\cdot y=0$, and $\mu_{\rm eff}B < d_{\rm eff}E$ in a large cylinder surrounding the z-axis. However, by adding magnetic field $\vec{B}=B_{\rm coil}\hat{z}$ along the centerline of the magnetic quadrupole with an external bias coil, a fully tunable scenario emerges.

Adding $B_{\rm coil}$ only slightly rounds the magnetic trapping potential, but it morphs the $\vec{E}\perp\vec{B}$ surface from a pair of planes into a hyperbolic sheet ($x\cdot y = z\cdot B_{\rm coil}/B'$),

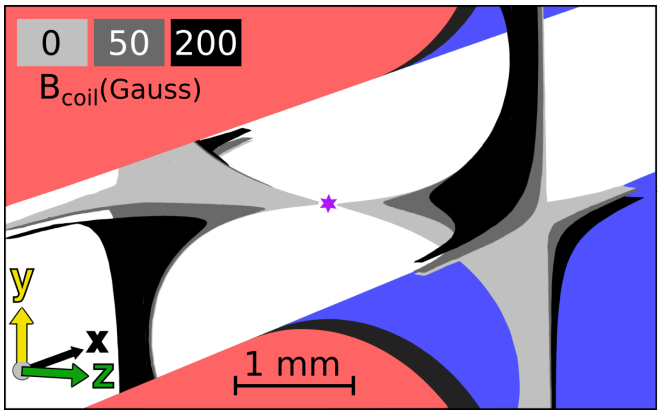

FIG. 3. Surfaces where spin-flips can occur ($\vec{E}\perp\vec{B}$, $\mu_{\rm eff}B<d_{\rm eff}E$) are shown for three values of $B_{\rm coil}$ in light gray, dark gray, and black. The magnetic pins are shown as in Fig. 2 for context. The purple star marks the trap center, to which molecules are confined within a ~1 mm diameter.

pushing it away from the z-axis where the magnetic field is smallest. Thus, small magnitudes of $B_{\rm coil}$ are sufficient to avoid loss. In Fig. 3, the surfaces where $\vec{E}\perp\vec{B}$ for several $B_{\rm coil}$ magnitudes are shown wherever the splitting is below the hopping threshold κ. The loss regions are tuned too far enough from the trap center that molecules cannot access them, yielding a striking difference in trap lifetime (Fig. 4a).

As a further confirmation of our model of the loss, we translate the magnetic pins along the $\hat{x}$ direction in their mounts to alter the surface where $\vec{E}\perp\vec{B}$, and compare experimental data against expectations (Fig. 4b). The translation serves to disrupt the idealized 2D magnetic quadrupole by adding a small trapping field $\vec{B}\propto B'z\hat{z}$. This means that $B_{\rm coil}$ no longer directly tunes the magnetic field magnitude along the z-axis. Instead, $B_{\rm coil}$ must first overcome the slight trapping field, translating a point of zero B-field along the z-axis and eventually out of the trap. This point has $\mu_{\rm eff}B<d_{\rm eff}E$ and $\phi=\vec{E}\cdot\vec{B}=0$, leading to strong loss unless aligned with the trap center where $E=0$ also. This means that without $B_{\rm coil}$, the loss should be a local minimum; as $|B_{\rm coil}|$ is increased the loss should first worsen and then improve when the zero leaves the trap. This qualitative explanation matches the observed double well structure in population verses $B_{\rm coil}$.

Quantitatively, we fit the family of curves (red, Fig. 4b) by assuming a completely time independent and thermal population distribution and integrating molecule flux weighted by Landau-Zener probability over the contorted surfaces where $\vec{E}\perp\vec{B}$ for each $B_{\rm coil}$ and pin translation. This idealized calculation nonetheless matches the data with only temperature as a free parameter, which fits to 170 ± 20 mK. [35].

We further confirm our model using microwave spectroscopy (Fig. 5), which detects the molecules experiencing a specific B-field by transferring them to an opposite

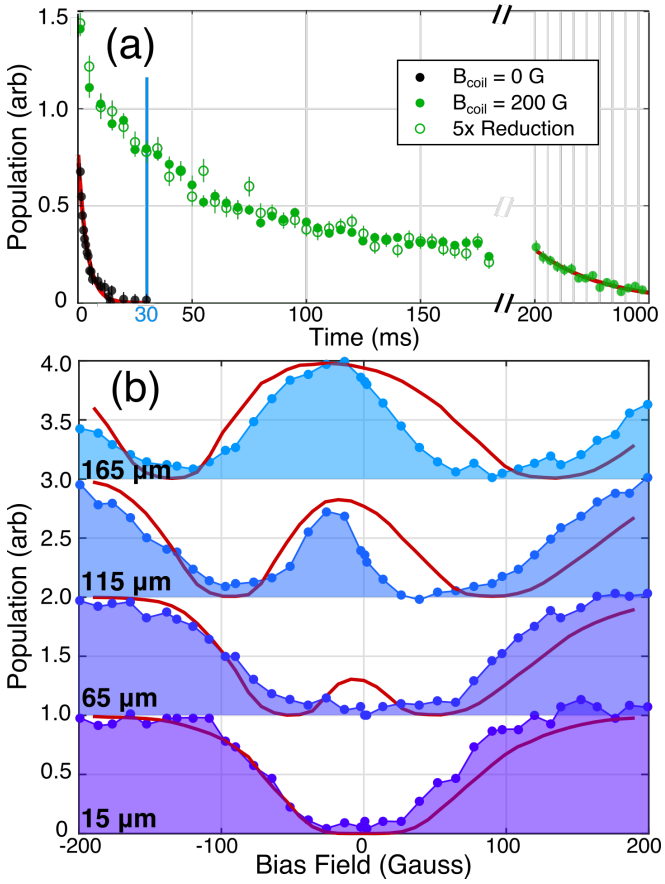

FIG. 4. Time traces (a) without bias field (black), with bias field (green dots), and with modulated density (green circles). One body fits (red) give loss rates of 200 s^{-1} without bias field and 2 s^{-1} with full bias field at long times, in agreement with our background gas pressure. At the fixed time 30 ms, population is shown as a function of both pin translation and bias field (b), for several values of pin translation, labeled relative to perfect alignment. Fits (red) are calculated by integrating the molecule flux of a thermal ensemble through surfaces where $\vec{E}\perp\vec{B}$.

parity state that is dark to our detection laser, as in [22]. Although the magnetic energy is only part of the total energy of molecules in our dual electric and magnetic quadrupole, molecules with a high magnetic energy during our spectroscopic snapshot are more likely to have a high total energy. It is seen that increasing $B_{\rm coil}$ increases population first at low fields and then at higher fields. This is consistent with our calculations showing that loss location moves further from the trap center with increasing $B_{\rm coil}$ (Fig. 3), and thus can be accessed only by higher energy molecules. At largest $B_{\rm coil}$ the distribution fits to 175 ± 15 mK, agreeing with the pin translation fits (Fig. 4b).

In the case of lowest applied B-field in Fig. 5, a negative signal is observed. This indicates an $|e\rangle$ state accumulation. Although the spin-flips we have discussed connect $|f,3/2\rangle$ to $|f,-3/2\rangle$, the latter experiences var-

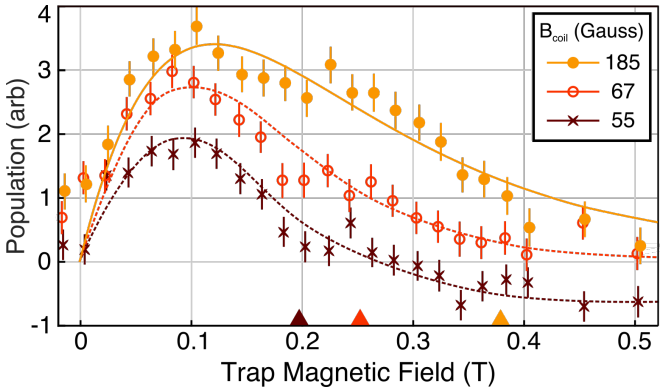

FIG. 5. Microwave spectroscopy shows that increasing B_{coil} increases population and shifts its distribution to higher energy. Triangles indicate the field at which a molecule can access loss regions for a given B_{coil}. The dotted lines are eye-guides, but the solid line for highest B_{coil} is a fit to 175 ± 15 mK.

ious avoided crossings due to the large electric confinement fields and remains weakly trapped. Its field-dressed state character varies, transitioning to $|e, 3/2\rangle$ at larger B-fields (Fig. 1d).

With loss removed, we observe a population trend whose initially fast decay rate decreases over time (Fig. 4a, green dots), suggesting collisions. To test this, we implement a five-fold reduction in initial population [36] and scale the resulting trend by five (green circles). If collisions had contributed, this new trend would show less decay, but we observe no significant change. This absence of collisions differs from our earlier work [22], which as we have mentioned shows signatures of evaporation for shallow cuts. This could be attributed to a significantly higher initial temperature and correspondingly lower density, reduced molecule number, or differences in trap geometry and loading. An alternative hypothesis for the population trend is the existence of chaotic trap orbits with long escape times [37]. Moving forward, we aim to increase the density by means of several improvements [38, 39].

Molecule enhanced spin-flip loss arises in mixed electric and magnetic fields due to a competition between field quantization axes where $\vec{E} \perp \vec{B}$ and $\mu_{\mathrm{eff}} B < d_{\mathrm{eff}} E$. We conclusively demonstrate this effect and overcome it using our dual magnetic and electric quadrupole trap. Our explanation of the effect provides detailed predictions of how its location and magnitude ought to scale with bias field and trap alignment, which we experimentally verify. Our results correct existing predictions about molecular spin-flips in mixed fields and pave the way toward further improvements in molecule trapping and cooling.

We acknowledge the Gordon and Betty Moore Foundation, the ARO-MURI, JILA PFC, and NIST for their financial support. T.L. acknowledges support from the Alexander von Humboldt Foundation through a Feodor Lynen Fellowship. We thank J.L. Bohn, S.Y.T. van de Meerakker, and M.T. Hummon for helpful discussions. We thank Goulven Quéméner for his continued involvement in this research.

* Contributed equally. Email dave.reens@colorado.edu or hao.wu@colorado.edu.
† Present Address: 5. Physikalisches Institut and Center for Integrated Quantum Science and Technology (IQST), Universität Stuttgart, Pfaffenwaldring 57, 70569 Stuttgart, Germany

[1] L. D. Carr, D. DeMille, R. V. Krems, and J. Ye, New Journal of Physics **11**, 055049 (2009).
[2] S. A. Moses, J. P. Covey, M. T. Miecnikowski, B. Yan, B. Gadway, J. Ye, and D. S. Jin, Science **350**, 659 (2015).
[3] T. Takekoshi, L. Reichsöllner, A. Schindewolf, J. M. Hutson, C. R. Le Sueur, O. Dulieu, F. Ferlaino, R. Grimm, and H.-C. Nägerl, Physical Review Letters **113**, 205301 (2014).
[4] J. W. Park, S. A. Will, and M. W. Zwierlein, Physical Review Letters **114**, 205302 (2015).
[5] M. Guo, B. Zhu, B. Lu, X. Ye, F. Wang, R. Vexiau, N. Bouloufa-Maafa, G. Quéméner, O. Dulieu, and D. Wang, Physical Review Letters **116**, 205303 (2016).
[6] L. R. Liu, J. T. Zhang, Y. Yu, N. R. Hutzler, Y. Liu, T. Rosenband, and K.-K. Ni, (2017), arXiv:1701.03121.
[7] B. K. Stuhl, B. C. Sawyer, D. Wang, and J. Ye, Physical Review Letters **101**, 243002 (2008).
[8] E. S. Shuman, J. F. Barry, and D. DeMille, Nature **467**, 820 (2010).
[9] M. T. Hummon, M. Yeo, B. K. Stuhl, A. L. Collopy, Y. Xia, and J. Ye, Physical Review Letters **110**, 143001 (2013).
[10] J. F. Barry, D. J. McCarron, E. B. Norrgard, M. H. Steinecker, and D. DeMille, Nature **512**, 286 (2014).
[11] V. Zhelyazkova, A. Cournol, T. E. Wall, A. Matsushima, J. J. Hudson, E. A. Hinds, M. R. Tarbutt, and B. E. Sauer, Physical Review A **89**, 053416 (2014).
[12] M. H. Steinecker, D. J. McCarron, Y. Zhu, and D. DeMille, ChemPhysChem **17**, 3664 (2016).
[13] B. Hemmerling, E. Chae, A. Ravi, L. Anderegg, G. K. Drayna, N. R. Hutzler, A. L. Collopy, J. Ye, W. Ketterle, and J. M. Doyle, Journal of Physics B: Atomic, Molecular and Optical Physics **49**, 174001 (2016).
[14] J. M. Doyle, J. D. Weinstein, R. DeCarvalho, T. Guillet, and B. Friedrich, Nature **395**, 148 (1998).
[15] H. L. Bethlem, G. Berden, and G. Meijer, Physical Review Letters **83**, 1558 (1999).
[16] J. R. Bochinski, E. R. Hudson, H. J. Lewandowski, G. Meijer, and J. Ye, Physical Review Letters **91**, 243001 (2003).
[17] E. Narevicius, A. Libson, C. G. Parthey, I. Chavez, J. Narevicius, U. Even, and M. G. Raizen, Physical Review Letters **100**, 093003 (2008).
[18] A. Wiederkehr, H. Schmutz, M. Motsch, and F. Merkt, Molecular Physics **110**, 1807 (2012).
[19] A. Prehn, M. Ibrügger, R. Glöckner, G. Rempe, and M. Zeppenfeld, Physical Review Letters **116**, 063005 (2016).
[20] Y. Liu, M. Vashishta, P. Djuricanin, S. Zhou, W. Zhong,

T. Mittertreiner, D. Carty, and T. Momose, Physical Review Letters **118**, 093201 (2017).
[21] L. P. Parazzoli, N. J. Fitch, P. S. Zuchowski, J. M. Hutson, and H. J. Lewandowski, Physical Review Letters **106**, 1 (2011).
[22] B. K. Stuhl, M. T. Hummon, M. Yeo, G. Quéméner, J. L. Bohn, and J. Ye, Nature **492**, 396 (2012).
[23] G. Quéméner and J. L. Bohn, Physical Review A - Atomic, Molecular, and Optical Physics **93**, 1 (2016).
[24] A. L. Migdall, J. V. Prodan, W. D. Phillips, T. H. Bergeman, and H. J. Metcalf, Physical Review Letters **54**, 2596 (1985).
[25] W. Petrich, M. H. Anderson, J. R. Ensher, and E. A. Cornell, Physical Review Letters **74**, 3352 (1995).
[26] K. B. Davis, M. O. Mewes, M. R. Andrews, N. J. van Druten, D. S. Durfee, D. M. Kurn, and W. Ketterle, Physical Review Letters **75**, 3969 (1995).
[27] B. K. Stuhl, M. Yeo, B. C. Sawyer, M. T. Hummon, and J. Ye, Physical Review A **85**, 033427 (2012).
[28] M. Lara, B. L. Lev, and J. L. Bohn, Physical Review A **78**, 033433 (2008).
[29] B. K. Stuhl, M. Yeo, M. T. Hummon, and J. Ye, Molecular Physics **111**, 1798 (2013).
[30] J. L. Bohn and G. Quéméner, Molecular Physics **111**, 1931 (2013).
[31] B. C. Sawyer, B. K. Stuhl, D. Wang, M. Yeo, and J. Ye, Physical Review Letters **101**, 203203 (2008).
[32] This is particularly relevant given the recently realized 3D MOT for YO.
[33] B. C. Sawyer, B. L. Lev, E. R. Hudson, B. K. Stuhl, M. Lara, J. L. Bohn, and J. Ye, Physical Review Letters **98**, 1 (2007).
[34] D. E. Pritchard, Physical Review Letters **51**, 1336 (1983).
[35] Calculation performed in COMSOL: Source Code.
[36] Microwaves couple opposite parities during deceleration, giving a uniform loss probability across the molecular distribution.
[37] R. González-Férez, M. Iñarrea, J. P. Salas, and P. Schmelcher, Physical Review E **90**, 062919 (2014).
[38] U. Even, EPJ Techniques and Instrumentation **2**, 17 (2015).
[39] Y. Segev, N. Bibelnik, N. Akerman, Y. Shagam, A. Luski, M. Karpov, J. Narevicius, and E. Narevicius, Science Advances **3**, e1602258 (2017).